Dual Templating of Macroporous Silicates with Zeolitic Microporous Frameworks

Brian T. Holland,[†] Lloyd Abrams,[‡] and Andreas Stein*,[†]

Department of Chemistry, University of Minnesota
Minneapolis, Minnesota, 55455
DuPont Central Research & Development
Contribution No. 7910, Wilmington, Delaware, 19880

Received February 10, 1999

This study reports the synthesis of silicates with bimodal pore structures of macropores (250 nm average diameter) that are surrounded by microporous silicalite walls. Dual templating methods are employed to control the hierarchical pore system. The macropores are formed by using arrays of monodisperse polystyrene (PS) spheres as templates, similar to a recently reported approach for the synthesis of highly ordered macroporous oxides,[1–4] aluminophosphates, and hybrid organosilicates.[5] The porosity of the walls is controlled by mixing a tetraethyl orthosilicate (TEOS) precursor with tetrapropylammonium hydroxide (TPAOH) as the structure-directing agent for silicalite walls (MFI structure). Materials with bimodal pore systems are of considerable interest for applications in catalysis and separations, since they combine the benefits of each pore size regime.[6–8] Micropores in zeolites provide size- or shape-selectivity for guest molecules;[9,10] channels in porous solids often impart the material with very high surface areas, which can increase host–guest interactions.[11] The microporous materials synthesized in this study contain additional macropores, which provide easier access to the active sites. Relatively short diffusion paths through the thin sample walls are expected to improve reaction efficiencies and minimize blocking of channels.

Previously, we reported that PS sphere templating with TEOS produced highly periodic macroporous silica structures with amorphous walls which contained a broad distribution of mesopores.[5] By pretreating the silica precursor with an aqueous mixture of cetyltrimethylammonium hydroxide and TPAOH, it was possible to tighten the mesopore size distribution significantly.[5] Similar meso/macroporous systems, templated with surfactant and polymer mixtures, have been reported recently.[2,8,12] In all of these structures the silica walls exhibited no crystalline domains. Bimodal pore structures involving zeolites are typically prepared by supporting zeolite crystallites on membranes[13] or by forming zeolite composites with other porous matrixes.[14] A synthesis of

a partially crystalline bimodal pore system with combined micro- and mesopores has recently been achieved by delaminating the layered zeolite MCM-22.[15] Attempts to crystallize the walls of mesoporous MCM-41 resulted in the formation of a material with increased catalytic activity; FTIR spectra revealed embryonic stages of tectosilicate formation, but PXRD patterns showed no crystalline features.[16] The walls in MCM-41 have a thickness of ~0.9–1.5 nm and can contain, at most, one layer of typical zeolite unit cells. Increasing the wall thickness would allow multiple unit cells, thus increasing crystallinity, stability and catalytic activity.

The walls in macroporous silicas synthesized by the PS sphere templating technique are typically tens of nanometers thick. The simplicity and generality of this technique make it viable for dual templating to form microporous walls. However, two potential problems needed to be addressed in designing a synthesis of macroporous zeolites. One challenge involved the crystallization kinetics of the walls. In preparations of other macroporous metal oxide compositions we observed that rapidly crystallizing oxides tended to result in large wall particles that were only tenuously connected. Typical hydrothermal zeolite preparations produce crystals that are micrometers in size. To limit the growth of crystals within the voids between latex spheres, it was necessary to employ conditions similar to those used in the synthesis of zeolite nanophase materials.[17] A greater challenge concerned the higher processing temperatures for hydrothermal syntheses of zeolites (100–200 °C), that tended to exceed the glass transition temperature of the PS spheres used as templates in our preparation ($T_g \approx 104$ °C).[18] To avoid phase separation or melting of spheres before a hard silica skeleton was formed, we employed a pseudo-solid-state transformation developed by Shimizu et al.[19] to convert preformed macroporous amorphous silica to silicalite.

PS spheres (526 ± 24 nm) were centrifuged at 1000 rpm (~100*g*) for 12 to 24 h to form close-packed arrays. The macroporous silicalite was synthesized by mixing 98% TEOS (24 mmol) with a 1.0 M aqueous solution of TPAOH (12 mmol) in a polyethylene (PE) bottle containing 2.0 g of the air-dried PS sphere arrays, and shaking for 10 min. The resulting composite was allowed to harden overnight in the capped PE bottle. The solid was then transferred to a Teflon-lined autoclave, where it was heated under autogenous pressure for 40 h at 130 °C (no solvent was added at this stage). During this process, the amorphous silica transformed into silicalite in the presence of the TPA⁺ structure-directing agent. The organic components were removed by calcination in air at 525 °C for 7 h to produce the macroporous silicalite **1**. The ²⁹Si MAS NMR spectrum of **1** showed a resonance centered at −114 ppm vs tetramethylsilane, which was attributed to Q⁴ silicons of silicalite. The Q⁴ envelope revealed shoulders due to the crystallographic inequivalent sites for Si in the silicalite framework.[20] Only a weak resonance (10% integrated intensity), attributable to Q³ silicons from surface hydroxyl groups or to an amorphous component, was observed at −104 ppm. The powder X-ray diffraction (PXRD) pattern of **1** (Figure 1) matched that of silicalite, with no evidence for another crystalline phase. The silicalite structure possesses two types of pores, straight channels along the [010] direction, formed by 10-membered rings (0.53 × 0.56 nm), and sinusoidal channels along the [100] direction, also composed of 10-membered rings (0.51

[†] University of Minnesota.

[‡] DuPont Central Research & Development.

(1) Velev, O. D.; Jede, T. A.; Lobo, R. F.; Lenhoff, A. M. *Nature* **1997**, *389*, 447–448.

(2) Velev, O. D.; Jede, T. A.; Lobo, R. F.; Lenhoff, A. M. *Chem. Mater.* **1998**, *10*, 3597–3602.

(3) Holland, B. T.; Blanford, C. F.; Stein, A. *Science* **1998**, *281*, 538–540.

(4) Wijnhoven, J. E. G. J.; Vos, W. L. *Science* **1998**, *281*, 802–804.

(5) Holland, B. T.; Blanford, C. F.; Do, T.; Stein, A. *Chem. Mater.* **1999**, *11*, 795–805.

(6) Davis, S. A.; Burkett, S. L.; Mendelson, N. H.; Mann, S. *Nature* **1997**, *385*, 420–423.

(7) Yang, H.; Coombs, N.; Ozin, G. A. *Adv. Mater.* **1997**, *9*, 811–814.

(8) Yang, P.; Deng, T.; Zhao, D.; Feng, P.; Pine, D.; Chmelka, B. F.; Whitesides, G. M.; Stucky, G. D. *Science* **1998**, *282*, 2244–2246.

(9) Breck, D. W. *Zeolite Molecular Sieves*; John Wiley & Sons: New York, 1974.

(10) Derouane, E. G.; Lenos, F.; Naccache, C.; Ribeiro, E. R. *Zeolite Microporous Solids: Synthesis, Structure and Selectivity*; Kluwer Academic Publishers: Dordrecht, 1992.

(11) Zhao, X. S.; Lu, G. Q.; Millar, G. J. *Ind. Eng. Chem. Res.* **1996**, *35*, 2075–2090.

(12) Antonietti, M.; Berton, B.; Göltner, C.; Hentze, H. P. *Adv. Mater.* **1998**, *10*, 154–159.

(13) Bein, T. *Chem. Mater.* **1996**, *8*, 1636–1653.

(14) Komarneni, S.; Katsuki, H.; Furuta, S. *J. Mater. Chem.* **1998**, *8*, 2327–2329.

(15) Corma, A.; Fornes, V.; Pergher, S. B.; Maesen, T. L. M.; Buglass, J. G. *Nature* **1998**, *396*, 353–356.

(16) Kloetstra, K. R.; van Bekkum, H.; Jansen, J. C. *Chem. Commun.* **1997**, 2281–2282.

(17) Ravishankar, R.; Kirschhock, C.; Schoeman, B. J.; Vanoppen, P.; Grobet, P. J.; Storck, S.; Maier, W. F.; Martens, J. A.; De Schryver, F. C.; Jacobs, P. A. *J. Phys. Chem. B* **1998**, *102*, 2633–2639.

(18) Wang, L. Ph.D. Thesis, University of Minnesota, Minneapolis, 1993.

(19) Shimizu, S.; Kiyozumi, Y.; Mizukami, F. *Chem. Lett.* **1996**, 403–404.

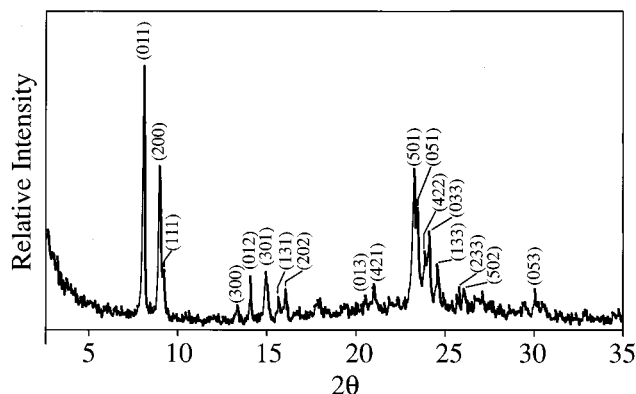(20) Fyfe, C. A.; O'Brien, J. H.; Strobl, H. *Nature* **1987**, *326*, 281–283.

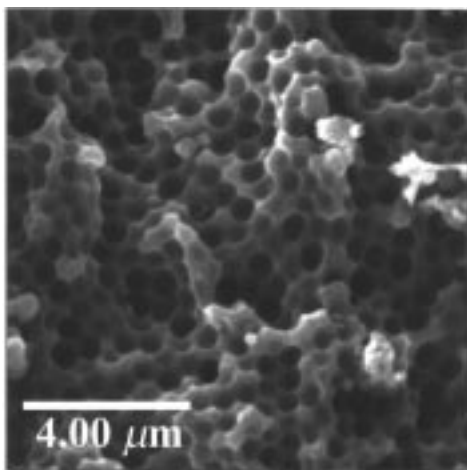**Figure 1.** PXRD pattern of **1**; *hkl* assignments were based on PDF file no. 44-696.

Figure 2. SEM image of **1**, showing the zeolitic walls around spheroidal voids that had been templated by polystyrene spheres.

× 0.55 nm).[21] The PXRD pattern was unchanged after the sample was refluxed in water for 13 h, indicating that the zeolitic walls were hydrothermally more stable than, for example, mesoporous silica with the MCM-41 structure.

FT-IR spectra of the macroporous silicalites were used for screening of the product phases. Absorptions occurred at 1224, 1106 (asymmetric Si−O stretch), 810 (symmetric Si−O stretch), 561/547 (doublet), and 453 cm^{-1} (Si−O bending vibration of internal silica tetrahedra[22]). The external asymmetric Si−O stretching vibration at 1224 cm^{-1} is only found in zeolites containing five-membered rings.[23] The band around 550 cm^{-1} has been assigned to the asymmetric stretching mode in five-membered ring blocks. Splitting of this lattice-sensitive band into a doublet has been observed in nanophase silicalite.[17] None of the calcined materials showed IR features of PS or the structure-directing molecules.

The scanning electron micrograph (SEM) of **1** (Figure 2) showed spheroidal voids with relatively uniform diameters (∼250 ± 30 nm). Typical macroporous particles had dimensions between 50 and 275 μm along the sides. No silicalite crystals extraneous to the macroporous solid were observed by SEM. The average wall thickness estimated from SEM measurements was 113 nm (range: 20−220 nm). The values overlap with average silicalite domain sizes (50−160 nm), estimated using the Scherrer equation and KBr powder as an internal reference. These wall thicknesses were smaller than those in typical ZSM-5 membranes[13] and
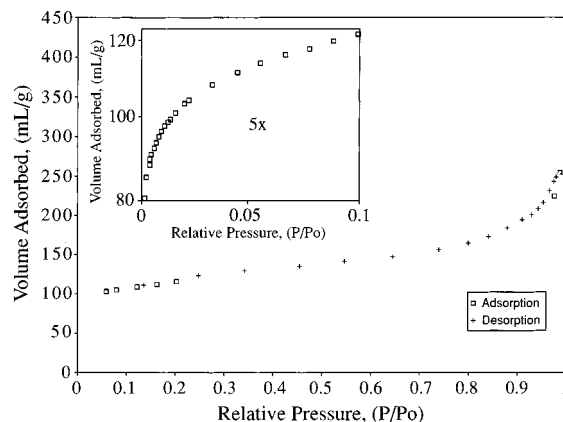
Figure 3. Nitrogen adsorption/desorption isotherms of **1**. The expanded adsorption isotherm (inset) demonstrates complete filling of the micropores at low partial pressures.

comparable to dimensions of silicalite nanophases,[17] resulting in short diffusion paths. Hg porosimetry measurements confirmed that the macropores were accessible. The surface area due to pores >3 nm was 52 m^2/g (corrected for sample compressibility), and the intrusion volume was 1.7 mL/g. The pore size distribution plot showed a bimodal distribution below 10 μm. Correlation with SEM indicated that a broad peak at 2.5 μm corresponded to cracks within particles, while a sharper peak around 174 nm correlated approximately with the templated macropores.

A type I N$_2$ adsorption/desorption isotherm (Figure 3) was indicative of microporosity in the material. A steep rise in uptake, followed by a flat curve at low relative pressures, corresponded to filling of micropores with N$_2$. The upward turn of the isotherm at higher relative pressures indicated filling of interparticle spaces. The total Brunauer−Emmett−Teller (BET) surface area of the sample was 421 m^2/g. Approximately half of this area was due to micropores, the other half was external to the micropores. A total single-point pore volume of 0.39 mL/g was measured. The calculated pore volume for pores >2 nm was 0.30 mL/g (Barrett−Joyner−Halenda (BJH)) or 0.27 mL/g (Digisorb). Both BJH and Digisorb calculations were based on the Kelvin equation, assuming a statistical N$_2$ coverage. The difference of ca. 0.1 mL/g could be attributed to the microporous component of the sample with pores <2 nm. For highly crystalline, dehydrated ZSM-5 the pore volume is approximately 0.2 mL/g.[24] The sorption data therefore indicated that the macroporous material was composed of silicalite walls with ∼50% crystallinity. The helium pycnometer density was 2.3 g/mL, typical for zeolites.

This study has demonstrated that macroporous silicalite can be synthesized by combining PS sphere templating with the use of an appropriate structure directing agent. Further incorporation of heteroatoms in the silica framework is expected to lead to catalytic or chromatographic supports with improved efficiencies, due to easier transport of guest molecules through the macropores and shorter diffusion pathways in the zeolitic walls. Detailed studies of the sorption behavior, thermal stability, and catalytic reactivities are currently underway.

Supporting Information Available: FT-IR and ^{29}Si MAS NMR spectra of **1** (PDF). This material is available free of charge via the Internet at http://pubs.acs.org.

JA990425P

(21) Meier, W. M.; Olson, D. H. *Atlas of Zeolite Structure Types*, 2nd ed.; Butterworth: Boston, 1987.

(22) Flanigen, E. M. *Zeolite Chemistry and Catalysis*; Rabo, J. A., Ed.; American Chemical Society: Washington, D.C., 1976; Vol. 171, pp 80−117.

(23) Jacobs, P. A.; Beyer, H. K.; Valyon, J. *Zeolites* **1981**, *1*, 161−168.

(24) Abrams, L.; Corbin, D. R. *J. Incl. Phenom. Mol. Recog.* **1995**, *21*, 1−46.